

# On the inhomogeneities of the sunspot penumbra

R. Schlichenmaier<sup>1,\*</sup>, D.A.N. Müller<sup>2</sup>, and C. Beck<sup>1,3</sup>

<sup>1</sup>Kiepenheuer-Institut für Sonnenphysik, Freiburg, Germany

<sup>2</sup>European Space Agency, c/o NASA Goddard Space Flight Center, Greenbelt, MD, USA

<sup>3</sup>Instituto de Astrofísica de Canarias, La Laguna, Tenerife, Spain

\*Email: schliche@kis.uni-freiburg.de

**Abstract.** The penumbra is ideally suited to challenge our understanding of magnetohydrodynamics. The energy transport takes place as magnetoconvection in inclined magnetic fields under the effect of strong radiative cooling at the surface. The relevant processes happen at small spatial scales. In this contribution we describe and elaborate on these small-scale inhomogeneities of a sunspot penumbra. We describe the penumbral properties inferred from imaging, spectroscopic and spectropolarimetric data, and discuss the question of how these observations can be understood in terms of proposed models and theoretical concepts.

## 1 Introduction

Almost hundred years ago, Hale (1908a,b) performed the first spectropolarimetric measurements on the Sun and discovered that sunspots are manifestations of magnetic fields with strengths of up to 3000 G in their centers. He proposed the tornado theory to explain both the darkness of a spot by dust that is whirled up into the solar atmosphere and the magnetic field by the circular current by electrons. Investigating Doppler shifts in sunspots, Evershed (1909) measured radial rather than circular movements in sunspot penumbrae and concluded that his findings were "entirely out of harmony with the splendid discovery of the Zeeman effect in sun-spots, made by Prof. Hale."

Until today, we lack a complete understanding of sunspots and penumbrae, but it seems obvious that the Evershed flow plays an essential role in the latter. The presence of the Evershed flow is intimately linked to the mere existence of the penumbra as demonstrated by the observations of Leka & Skumanich (1998). The filamentary bright and dark structure should be related to the flow field, in a similar way as the granular pattern of the quiet Sun is related to the granular flow field of hot up- and cool downflows.

The magnetic field can – in principle – be inferred from the spectropolarimetric imprints of the Zeeman effect on photospheric absorption lines. However, this leads to unambiguous results only if the magnetic and velocity fields are homogeneous along the line-of-sight. Considerable complications in interpreting the line profiles arise if gradients or discontinuities are present in the volume of the solar atmosphere which is sampled by one resolution element. Such variations may be present laterally due to insufficient spatial resolution, but also along the line-of-sight from the depth layers that contribute to the observed line profile.

In this contribution, we make the case that the latter must be assumed to reconstruct some of the observed profile asymmetries. We summarize our knowledge of the inhomogeneities in the magnetic and velocity field of a sunspot penumbra, aiming at an understanding of radiative magneto-convection in inclined magnetic fields.

## 2 Penumbral properties

The photospheric penumbral properties may be characterized by three different types of measurements: (1) imaging, (2) spectroscopy of lines that do not show the Zeeman effect, and (3) spectropolarimetric measurements of Zeeman sensitive lines.

### 2.1 Imaging

At a spatial resolution of  $1''$  or worse, the penumbra appears as a gray ring that surrounds the umbra. The radial bright and dark filaments only become apparent at a spatial resolution of about  $0.5''$ . At a spatial resolution of about  $0.2''$  bright filaments show internal intensity variations: In the inner penumbra, predominantly on the center side, bright filaments show a dark elongated core (Scharmer et al. 2002; Sütterlin et al. 2004; Langhans et al. 2007). Such dark-cored bright filaments have a width of some  $0.2''$ .

### 2.2 Spectroscopy

As for the intensity, the length scale of variations in a Doppler map decreases with improving spatial resolution. At  $1''$  no flow filaments are visible and the Doppler shifts only show a transition from red shifts on the limb side to blue shifts on the center side. To infer the flow vector at this spatial resolution, azimuthal cuts at constant distance from the spot center are constructed. The azimuthal mean reflects the vertical velocity component, while the amplitude of the variation measures the horizontal component which is known to be dominant. It is found that the flow field has an upward component in the inner and a downward component in the outer penumbra (Schlichenmaier & Schmidt 2000; Schmidt & Schlichenmaier 2000).

A filamentary structure becomes visible in velocity maps of the penumbra if the spatial resolution is of the order of  $0.5''$  or better. However, flow filaments are not always co-spatial with intensity filaments (Tritschler et al. 2004; Schlichenmaier et al. 2005). Individual flow and intensity filaments typically have a joined starting point in the inner penumbra. Yet, further outwards the flow filament is not always co-spatial with a bright filament.

The Evershed flow in the penumbra is characterized not only by a line shift, but also by a line asymmetry. The line asymmetry is such that the wing is more strongly shifted than the core (Bumba 1960; Schröter 1965a; Wiehr et al. 1984; Degenhardt 1993; Wiehr 1995). The asymmetry decreases with formation height of the spectral line (Degenhardt & Wiehr 1994; Balthasar et al. 1997). Studying the line asymmetry, i.e., the shape of the bisector, one can show that the measurements are consistent with the assumption that the flow is concentrated in the deepest photospheric layers (Maltby 1964). Line asymmetries could in principle be assigned to laterally separated unresolved components (Schröter 1965b), but as they are still present in high spatial resolution observations down to  $0.3''$  (see Bellot Rubio et al. 2005), the line asymmetries can only be explained by velocity gradients or discontinuities

along the line-of-sight (Schlichenmaier et al. 2004; Bellot Rubio et al. 2006). Therefore, the measurements seem to require a flow field that is concentrated in the deepest layers of the photosphere beneath  $\tau \approx 0.1$ .

Spectroscopy at  $0''.3$  spatial resolution resolves dark-cored bright filaments. Bellot Rubio et al. (2005) found that the dark cores are associated with strong predominantly horizontal flows, while the lateral bright edges are less Doppler shifted. Yet the lateral bright edges are still more shifted than the dark surroundings in which the dark-cored penumbral filaments are often embedded in the inner penumbra. The inner end of a dark-cored bright filament is typically bright and is associated with an upflow. Rimmele & Marino (2006) find that these hot upflows have a diameter of about  $0''.3$  and turn horizontal within  $1''$ . They continue in the dark core of a bright filament.

### 2.3 Magneto-convective modelling

The first attempt to describe quantitatively (i) the dynamic evolution of penumbral filaments and (ii) the Evershed effect consisted of a 1D (thin) magnetic flux tube that evolved in a 2D time-independent background (Schlichenmaier et al. 1998a,b). Such tubes develop a flow that brings up hot plasma into the photosphere which radiatively cools as it flows outwards, yielding a flow topology that is consistent with the findings by Rimmele & Marino (2006). As long as the plasma is hot, the magnetic field strength is reduced and can be weaker by  $10^3$  G as compared to the background. In this framework, magneto-convective instabilities cause solutions in the form of sea serpents (Schlichenmaier 2002), in which the hot upflow is followed by a cool downflow further outwards. Such a flow arch is conceptually very similar to the time-independent siphon flows (e.g., Degenhardt 1991; Thomas & Montesinos 1993). In both cases a pressure gradient accelerates the flow. The pressure gradient in the moving tube model is sustained by radiative cooling between the inner hot footpoint (high gas pressure) and the cool flow channel further outwards (low gas pressure). This configuration is a natural consequence of magneto-convective instabilities and radiative cooling.

In contrast, Weiss et al. (2004) have proposed that magnetic field lines associated with the downflows in the outer penumbra are pumped downwards by small-scale granular convection outside the sunspot. They demonstrate that turbulent transport of mean magnetic fields by convective motions, i.e., magnetic pumping, is a robust phenomenon. However, in this scenario it remains obscure how the magnetized penumbra with supposedly coherent flows and field lines is connected to the turbulent convection that is needed to produce topological pumping effects. It seems more promising to perform 3D simulations of inclined magnetoconvection including the effects of radiation. First results have been presented by Heinemann et al. (2006) which confirm the flow topology that we describe above of a hot upflow followed by a cooler downflow (cf. their Fig. 6). Yet, in these simulations the flow is not strictly radial, but has a small azimuthal component towards the lateral edges of the filament. Eventually such simulations will clarify whether or not the energy transport takes place due to convection in field free gaps as it was suggested recently (Spruit & Scharmer 2006; Scharmer & Spruit 2006) or by flows along magnetic tubes as suggested by the moving tube model. In any model, the magnetic field strength in bright penumbral features is certainly less than 1000 G, i.e., much smaller than the average surrounding magnetic field strength. In accordance with the latter expectation, Bellot Rubio et al. (2005) measure that dark-cored filaments have smaller magnetic field strengths than the surroundings of the fil-

Stokes V profiles along trace from  
outer (bottom) to inner (top) penumbra.  
Unit of y-axis: V/I in %.

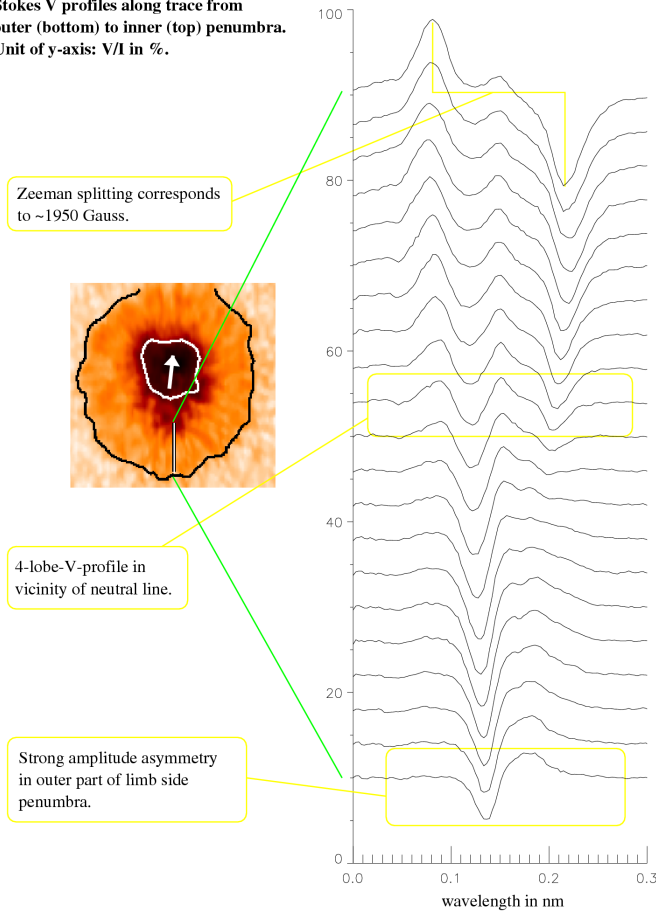


**Figure 1.** Stokes-V profiles of Fe I 1564.8 nm along a radial cut for the limb-side penumbra of a spot at 30° heliocentric angle. From the inner to the outer penumbra, the V-profiles undergo a transition from one polarity to the other. In the central penumbra, along the so-called magnetic neutral line, both polarities seem to be present. This is clear observational evidence for an inhomogeneous magnetic field. Such a 4-lobe-profile needs at least two different orientations of the magnetic field within one resolution element.

aments. They use the Zeeman sensitive line Fe II 6149 nm and even find a tendency that the strength is slightly larger in dark cores than in the bright lateral edges, as one expects due to contraction of the plasma during the cooling phase.

## 2.4 Spectropolarimetry

Spectroscopic measurements establish the inhomogeneous flow field within the sunspot penumbra. Direct observational evidence for an inhomogeneous magnetic field consists of 4-lobe V-profiles as presented in Fig. 1: At the location within the penumbra where the viewing angle to the average magnetic field lines is perpendicular, i.e., in the vicinity of the magnetic neutral line, one expects vanishing V-signal if the field were homogeneous. V-profiles with up to four lobes, as observed, imply that at least two directions (components) of the magnetic field must be present in the resolution element. Another strong indication of non-trivial topologies of the velocity and magnetic field are given by the observations of amplitude and area asymmetries of Stokes-V (e.g., Sánchez Almeida & Lites 1992; Schlichenmaier &

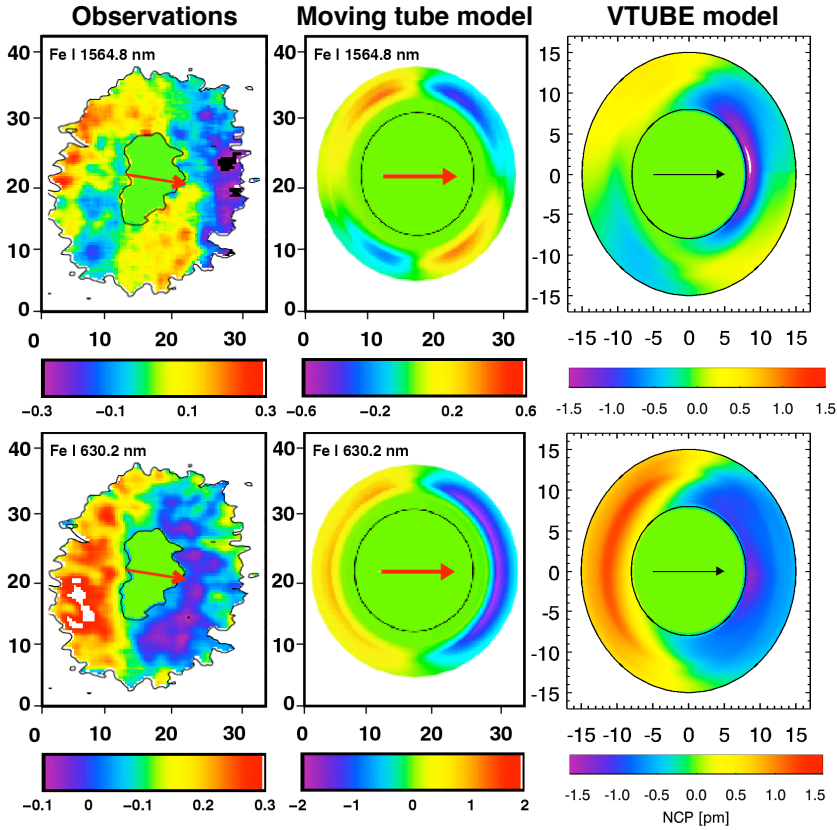


**Figure 2.** Observed and synthesized sunspot maps of net circular polarization for Fe I 15648 nm (top row) and Fe I 630.2 nm (bottom row), respectively. The synthesized maps in the middle column are based on a snapshot from the moving tube model (Müller et al. 2002), and the maps in the right column are based on the VTUBE tool (see text), where inversion results are used. The spot is at a heliocentric angle of  $30^\circ$  and the arrows point towards disk center.

Collados 2002). These findings motivate that reconstructions of the (magnetic and velocity) field topology should consider at least two components or strong gradients or discontinuities along the line-of-sight. Such attempts have been made using inversion techniques (e.g., Belot Rubio et al. 2004; Borrero et al. 2006). In such inversions, synthetic Stokes parameters resulting from polarized radiative transfer based on model atmospheres are compared with observed profiles of the four Stokes parameters.

The assumption of two interlaced components with constant velocity and magnetic fields give reasonable fits to the observed profiles. Yet, the pure existence of net circular polarization,  $\mathcal{N} = \int V(\lambda) d\lambda$ , proves that velocity gradients along the line-of-sight are present (Sánchez Almeida & Lites 1992; Landolfi & Landi degl’Innocenti 1996). Sunspot maps of the net circular polarization are displayed in Fig. 2. The first row shows observed and synthesized maps of Fe I 15648 nm, and the second row shows the same for Fe I 630.2 nm. The

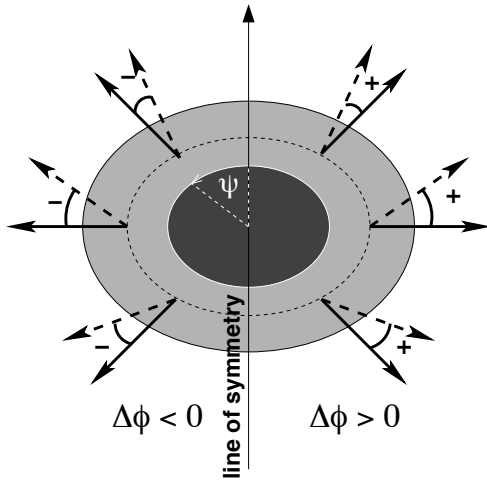


**Figure 3.** Difference in the azimuth,  $\Delta\phi$ , of horizontal and inclined magnetic field when viewed off disk center. The sign of  $\Delta\phi$  changes from one side of the penumbra to the other. The dashed vectors represent the less inclined background magnetic field being at rest, and the solid vectors represent the horizontal magnetic components that is coaligned with the flow.

observed maps of  $\mathcal{N}$  (left column) are simultaneous measurements of the same sunspot at  $30^\circ$  heliocentric angle (Müller et al. 2006). The symmetry properties of the two observed maps are different. The middle column shows synthetic maps that are based on a snapshot of the moving tube model (Müller et al. 2002). The synthetic maps reproduce the observations quite convincingly. The main ingredient for reproducing these symmetry properties are two components along the line-of-sight with the following properties (1) They have two different inclinations of the magnetic field and (2) they are Doppler shifted relative to each other (Schlichenmaier et al. 2002). Figure 3 sketches how the two different inclinations of the magnetic field produce a sign change in the difference of the magnetic field azimuth, which is crucial to reconstruct the observed maps. It is important to realize that these maps cannot be reproduced with a mixture of two laterally separated (unresolved) components with each having constant magnetic and velocity fields along the line-of-sight!

### 3 A diagnostic tool: VTUBE

In an attempt to bring together snapshots from simulations and results from inversions, a tool to diagnose spectropolarimetric measurements was developed (Müller et al. 2006). We constructed a 3D geometric model (VTUBE) of a magnetic flux tube embedded in a background atmosphere that can be used to gain a better understanding of the different factors that determine  $\mathcal{N}$  and its spatial variation within the penumbra. This model serves as the frontend for a radiative transfer code (DIAMAG, Grossmann-Doerth 1994). Combining the two, we can generate synthetic Stokes spectra for any spectral line and construct maps of suited diagnostic quantities, like  $\mathcal{N}$ -maps, for any desired axisymmetric magnetic field configuration and arbitrary properties of flux tubes being embedded in an arbitrary atmosphere. The model has been built to offer a high degree of versatility, e.g. the option to calculate several parallel rays along the line-of-sight that intersect the tube at different locations with arbitrary viewing angles. One can then average over these rays to model observations of flux tubes at different spatial resolutions and for different magnetic filling factors of the atmosphere. Furthermore, one can also take into account radial variations of the physical properties of the flux tube.

Doing so, one can e.g. model the interface between the flux tube and its surroundings.

To generate a realistic  $\mathcal{N}$ -map with the VTUBE model, we extracted the radial dependence of azimuthally averaged quantities from results of inversions based on two components as mentioned above, thereby assuming that the penumbral fine structure is axially symmetric. From the two components, one is assigned to be the background component, and the other serves as the flow component. This is in accordance with inversion results with one component being essentially at rest and the other the other carrying the flow. While the magnetic field strength decreases with penumbral radius, the difference between the weaker flow component and the stronger one decreases outwards and vanishes at the outer penumbral edge. The flow velocity along the channel (flow component) increases from some 6 km/s at the inner to 8 km/s in the outer penumbra. The inclination of the flow changes gradually from an upflow with  $20^\circ$  in the inner to a downflow with  $-10^\circ$  in the outer penumbra. The resulting maps (right column in Fig. 2) compare well with the observed ones, but, especially in the radial dependence, differences are seen. Possibly this difference may be explained by recent results (Bellot Rubio et al. 2003; Beck 2006) that suggest that the background field is not at rest in the outermost penumbra, but shows flow velocities of up to 1 km/s. This may modify the  $\mathcal{N}$ -map and may reconcile the model with the observations.

## 4 Conclusions

We have described the properties of a sunspot penumbra, including the topology of the magnetic and velocity field. The main conclusion is that the penumbra is inhomogeneous. In order to explain the mentioned spectroscopic and spectropolarimetric measurements at least strong gradients if not discontinuities must be present along the line-of-sight. We believe that low lying channels ( $\tau > 0.1$ ) that carry a magnetized flow and are embedded in a magnetized background at rest must be assumed in order to understand the measurements, like the observed bisectors of unmagnetic lines, and the symmetry properties of net-circular-polarization maps. Yet, we cannot offer a complete picture as the spatial resolution is not yet good enough to present unambiguous model fits to the observed spectropolarimetric measurements. A great step forward may be accomplished by the recently launched satellite Hinode, as it will allow for spectropolarimetric observations at  $0''.25$ . The best ground based observations today are not much better than  $1''$ . At the same time, simulations of magneto-convection in inclined magnetic field like the ones presented recently by Heinemann et al. (2006) will significantly enhance our understanding of the penumbral fine structure.

## References

- Balthasar, H., Schmidt, W., & Wiehr, E. 1997, *Solar Phys.* 171, 331
- Beck, C. 2006, PhD thesis, Universität Freiburg (Kiepenheuer-Institut für Sonnenphysik)
- Bellot Rubio, L. R., Balthasar, H., & Collados, M. 2004, *A&A*, 427, 319
- Bellot Rubio, L. R., Balthasar, H., Collados, M., & Schlichenmaier, R. 2003, *A&A*, 403, L47
- Bellot Rubio, L. R., Langhans, K., & Schlichenmaier, R. 2005, *A&A*, 443, L7
- Bellot Rubio, L. R., Schlichenmaier, R., & Tritschler, A. 2006, *A&A*, 453, 1117
- Borrero, J. M., Solanki, S. K., Lagg, A., Socas-Navarro, H., & Lites, B. 2006, *A&A*, 450, 383
- Bumba, V. 1960, *Izv. Krymk. Astrofiz. Observ.*, 23, 253
- Degenhardt, D. 1991, *A&A*, 248, 637

- Degenhardt, D. 1993, A&A, 277, 235
- Degenhardt, D. & Wiehr, E. 1994, A&A, 287, 620
- Evershed, J. 1909, MNRAS, 69, 454
- Grossmann-Doerth, U. 1994, A&A, 285, 1012
- Hale, G. E. 1908a, ApJ, 28, 315
- Hale, G. E. 1908b, ApJ, 28, 100
- Heinemann, T., Nordlund, A., Scharmer, G. B., & Spruit, H. C. 2006, ArXiv Astrophysics e-prints, astro-ph/0612648
- Landolfi, M. & Landi degl'Innocenti, E. 1996, Solar Phys. 164, 191
- Langhans, K., Scharmer, G. B., Kiselman, D., & Löfdahl, M. G. 2007, A&A, accepted
- Leka, K. D. & Skumanich, A. 1998, ApJ, 507, 454
- Maltby, P. 1964, Astrophysica Norvegica, 8, 205
- Müller, D. A. N., Schlichenmaier, R., Fritz, G., & Beck, C. 2006, A&A, 460, 925
- Müller, D. A. N., Schlichenmaier, R., Steiner, O., & Stix, M. 2002, A&A, 393, 305
- Rimmele, T. & Marino, J. 2006, ApJ, 646, 593
- Sánchez Almeida, J. & Lites, B. W. 1992, ApJ, 398, 359
- Scharmer, G. B., Gudiksen, B. V., Kiselman, D., Löfdahl, M. G., & Rouppe van der Voort, L. H. M. 2002, Nature, 420, 151
- Scharmer, G. B. & Spruit, H. C. 2006, A&A, 460, 605
- Schlichenmaier, R. 2002, AN, 323, 303
- Schlichenmaier, R., Bellot Rubio, L. R., & Tritschler, A. 2004, A&A, 415, 731
- Schlichenmaier, R., Bellot Rubio, L. R., & Tritschler, A. 2005, Astron. Nachr., 326, 301
- Schlichenmaier, R. & Collados, M. 2002, A&A, 381, 668
- Schlichenmaier, R., Jahn, K., & Schmidt, H. U. 1998a, ApJL, 493, L121
- Schlichenmaier, R., Jahn, K., & Schmidt, H. U. 1998b, A&A, 337, 897
- Schlichenmaier, R., Müller, D. A. N., Steiner, O., & Stix, M. 2002, A&A, 381, L77
- Schlichenmaier, R. & Schmidt, W. 2000, A&A, 358, 1122
- Schmidt, W. & Schlichenmaier, R. 2000, A&A, 364, 829
- Schröter, E. H. 1965a, Z. Astrophys., 62, 228
- Schröter, E. H. 1965b, Z. Astrophys., 62, 256
- Spruit, H. C. & Scharmer, G. B. 2006, A&A, 447, 343
- Sütterlin, P., Bellot Rubio, L. R., & Schlichenmaier, R. 2004, A&A, 424, 1049
- Thomas, J. H. & Montesinos, B. 1993, ApJ, 407, 398
- Tritschler, A., Schlichenmaier, R., Bellot Rubio, L. R., & the KAOS Team 2004, A&A, 415, 717
- Weiss, N. O., Thomas, J. H., Brummell, N. H., & Tobias, S. M. 2004, ApJ, 600, 1073
- Wiehr, E. 1995, A&A, 298, L17
- Wiehr, E., Koch, A., Knölker, M., Küveler, G., & Stellmacher, G. 1984, A&A, 140, 352